

WAVEGUIDE TYPE OPTICAL ISOLATOR USING FARADAY AND COTTON-MOUTON EFFECTS IN BI-SUBSTITUTED YIG THIN FILMS

YASUMITSU MIYAZAKI, KAZUNARI TAKI and YASUO AKAO

Department of Electrical Engineering

(Received July 4, 1981)

Abstract

Propagation and mode conversion properties of optical waves in film waveguides made of magneto-optic materials such as garnet crystals are studied in order to construct optical thin film isolators using magneto-optic effects. Gyrotropic YIG films are fabricated on GGG crystal substrates by RF sputtering method. Faraday effects in gyrotropic film waveguides are investigated for non-reciprocal guide parts of optical film devices. Magneto-optic Cotton-Mouton effects are also studied for reciprocal parts of optical devices. Birefringence effects in sputtered garnet films that are very useful for mode matching are found. By using ferrite magnets for external magnetic fields thin film type optical isolators of total lengths of 3.3–4.6 mm, consisting of Bi-substituted YIG films, are constructed. Isolation ratio of the isolator for forward and backward optical waves is 7.5 dB.

CONTENTS

| | |
|--|----|
| 1. Introduction | 43 |
| 2. Structure of optical isolator | 43 |
| 3. Characteristics of sputtered Bi:YIG thin-films | 44 |
| 4. Mode conversion properties in Bi:YIG thin-film waveguides | 45 |
| 4. 1. Propagation losses | 46 |
| 4. 2. Mode conversions due to Faraday effects..... | 46 |
| 4. 3. Mode conversions due to Cotton-Mouton effects..... | 47 |
| 5. Optical isolation in the Bi:YIG film waveguide | 49 |
| 6. Birefringence effects on the mode conversions | 50 |
| 7. Conclusion..... | 55 |

1. Introduction

Thin-film optical devices using magneto-optic effects, such as modulators¹⁾, switches²⁾ and isolators^{3~5)}, have been investigated for laser communication systems by many authors.

In thin-film optical devices, guided optical waves are focussed in film waveguides of small cross-sections. Intensive external electric, magnetic and acoustic fields can be obtained in small local regions of the film wave guides by using weak electric powers. These properties lead to effective strong interactions between optical waves and external fields.

An optical isolator is one of the optical devices that have not been fabricated as far. In this paper, an optical film isolator, that is one of the general optical devices and constructed from non reciprocal and reciprocal guide sections, is discussed.

Waveguide type optical isolators are important as unidirectional waveguides and are indispensable for stabilization of laser oscillation and separation of optical waves in integrated optical circuits. However, waveguide type optical isolators with sufficient properties have not been realized since there are some difficulties to the fabrications^{3,6)}. The authors have shown the analysis on hybrid modes for the case of optical modulators using the Kerr effects⁷⁾ and nonreciprocal circuits of optical isolators using the Faraday effect in gyrotropic garnet films with isotropic ZnO and anisotropic LiIO₃ top layers for accomplishing mode matching^{8,9)}. In order to construct optical isolators, in these constructions anisotropic crystals are required for reciprocal circuits. However, it is difficult to grow anisotropic single crystals on garnet films that are almost isotropic. From a fabrication point of view, the Cotton-Mouton effect of gyrotropic films is very useful for reciprocal circuits⁴⁾.

The authors have fabricated YIG¹⁰⁾ and Bi-substituted YIG (Bi:YIG) single crystal films¹¹⁾ of relatively good quality on GGG substrates by RF sputtering method. In this paper, propagation properties of optical waves in the garnet films are studied. TE-TM mode conversions due to the Faraday and the Cotton-Mouton effects are measured in Bi:YIG single crystal films sputtered on GGG substrates. From the experimental results, the design data for nonreciprocal and reciprocal circuits of waveguide type optical isolators are determined, such as propagation length and applied magnetic fields. Furthermore, by using ferrite magnets a waveguide type optical isolator is constructed practically with short propagation length and small magnetic external fields, and nonreciprocal properties are measured. In order to obtain optimum design data for waveguide type optical isolators, comparing with experimental results, theoretical calculations are performed, with consideration of weak birefringences in Bi:YIG thin-films¹²⁾ resulting from the misfit stress. It is shown that waveguide type optical isolators can be constructed in forms of very small integrated circuits, with mode degeneracy induced by the birefringence.

2. Structure of Optical Isolator

A basic structure of a waveguide type optical isolator⁹⁾ is shown in Fig. 1. This isolator has three sections of mode selector, non reciprocal and reciprocal

mode converters. This isolator consists of a Bi-substituted YIG (Bi:YIG) thin-film sputtered on a GGG substrate and a ZnO for the top layer. The thickness of Bi:YIG and ZnO are $2.15 \mu\text{m}$ and $1 \mu\text{m}$, respectively. The refractive index of GGG substrate is 1.945 at the wavelength $\lambda=1.15 \mu\text{m}$ and that of Bi:YIG film without external magnetic field is 2.18. The refractive index $n=1.945$ of ZnO is approximately equal to that of GGG. In the nonreciprocal circuit, the Faraday effect in the Bi:YIG gyrotropic film produces a nonreciprocal TE-TM mode conversion, where the magnetization of the garnet film is parallel to the propagation direction of optical wave. In the reciprocal circuit, Cotton-Mouton effect is used for a reciprocal mode conversion, where the magnetization is transverse to the propagation direction and at an angle of θ with the normal line to the film plane. The TE-TM mode conversion efficiency of 50% is required for the reciprocal and nonreciprocal circuits in the optical isolator, respectively. The ZnO top layer can yield the 50% mode conversion with smaller thickness of garnet film, comparing with the case of the air top layer. The ZnO top layer also protects the optical guide from the lossy effects of external magnetic circuit parts as buffer layers^{9,13}. The mode selector of aluminium clad waveguide attenuates only TM modes¹⁴.

In this structure, since optical waveguide have not discontinuities, there is no connection loss at the boundary between the nonreciprocal and the reciprocal circuits. The film thickness and propagation length in this Bi:YIG film isolator are very small compared with the optical isolators with YIG thin-films. Furthermore, the fabrication of this isolator by RF sputtering method is very easy, because no anisotropic single crystal is required for the the top layer in non reciprocal and reciprocal parts. External magnetic field can also be obtained by sputtered ferrite films on the ZnO top layer.

3. Characteristics of Sputtered Bi:YIG Thin-films

For the gyrotropic thin-films of optical isolators, Bi:YIG thin-films are used because of large magneto-optic effects. Using Bi:YIG targets, Bi:YIG films are fabricated on GGG crystal substrates by RF sputtering method which has fine film-thickness control and reproducibility¹¹.

The sputtering conditions are shown in Table 1. Substrates are heated to 750°C and RF power is 85 W. Gas pressures of Ar and O_2 are 4×10^{-4} and 1×10^{-4} Torr, respectively, growth rates of garnet films are 850 \AA/hr . The composition of the sputtering target is $\text{Bi}_1\text{Y}_2\text{Fe}_4\text{Al}_1\text{O}_{12}$. In the target, Fe is substituted by Al in order to reduce the mismatch in lattice constant between the Bi:YIG thin-film and the GGG substrate, and the optical absorption. The optical and magnetic properties of the sputtered Bi:YIG films of thickness $d=2.13 \mu\text{m}$ are summarized

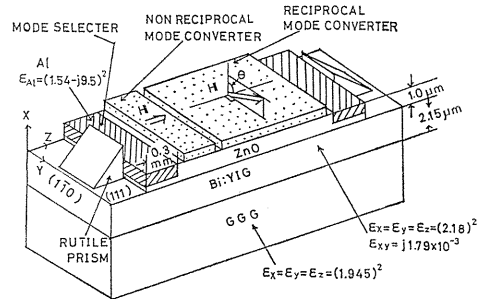


Fig. 1. Basic structure of the waveguide type optical isolator.

Table 1. Sputtering conditions of Bi:YIG films.

| | |
|-----------------------|--|
| Target | $\text{Bi}_1\text{Y}_2\text{Fe}_4\text{Al}_1\text{O}_{12}$ |
| RF Power | 85 W |
| Sputtering Gasses | Ar 4×10^{-4} Torr |
| | O ₂ 1×10^{-4} Torr |
| Substrate Temperature | 750°C |
| Deposition Rate | 850 Å/hr |

Table 2. Optical and magnetic properties of Bi:YIG films.

| | | |
|---------------------------|----------------|------------------------|
| Refractive index | (n) | 2.18 |
| Specific Faraday rotation | (θ_F) | 460 [deg./cm] |
| Absorption coefficient | (α) | 2 [cm ⁻¹] |
| Saturation magnetization | ($4\pi M_s$) | 90.5 [G] |
| Coercive force | (H_c) | 3 [Oe] |
| Thickness | (d) | 2.13 [μm] |

in Table 2. The refractive index measured by Abelés method is 2.18 and the magnetic properties were obtained by vibrating sample magnetometer (VSM). The saturation magnetization is 90.5 G and the coercive force is 3 Oe. The specific Faraday rotation $\theta_F=460$ (deg./cm) was determined from the experimental results of the TE-TM mode conversion as shown in next section. The quality of crystallization were evaluated by the Xray diffractometer and Laue method. Only (444) diffraction line was obtained from the Xray-diffractometer. In the measurement

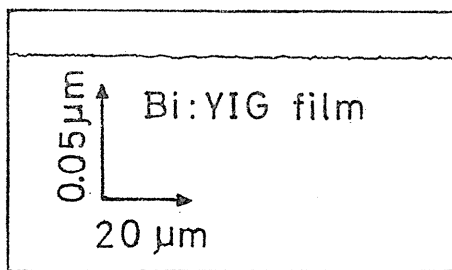


Fig. 2. Surface of sputtered Bi:YIG films.

of Laue method with inclined incident Xray, only Laue spots appeared. No halo and Debye-Scherrer ring concerned with properties of polycrystals and amorphous materials were confirmed from Laue method. These facts indicate that the sputtered Bi:YIG thin-films on GGG substrates are single crystals. The roughnesses of the film surfaces are about 30 Å as shown in Fig. 2, so that these Bi:YIG films have small scattering losses and can be used as optical waveguides.

4. Mode Conversion Properties in Bi:YIG Thin-film Waveguides.

The experimental set-up for the measurement of TE-TM mode conversions in Bi:YIG thin-film waveguides is shown in Fig. 3, where B.S. is a beam splitter. The sample is placed on the goniometer table. The optical wave radiated from a

He-Ne laser of the wavelength $1.15 \mu\text{m}$ is linearly polarized as the TE wave through the polarizer and fed into the Bi:YIG thin-film waveguide by a rutile prism. A pair of rutile right-angle prisms, of which refractive indices are $n_e=2.725$ and $n_o=2.470$, are used as input and output couplers. The guided wave is coupled out of the waveguide by the output prism and after through the analyzer detected by a PbS photoconductive cell. The cell has been checked for the linear characteristics.

The output voltage of the PbS cell is measured by the pen recorder through the lock-in amplifier. The He-Ne laser of $0.633 \mu\text{m}$ is used for the alignment of optical axis, because $1.15 \mu\text{m}$ He-Ne laser is invisible. External magnetic fields are applied by using a solenoid coil in the case of measurement of the Faraday effect and by using an electromagnet with two poles in the case of measurement of the Cotton-Mouton effect¹⁵⁾.

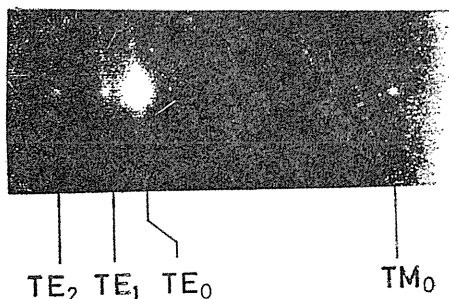


Fig. 4. Guided modes excited by a He-Ne laser.

than the ordinary index for TM modes, the coupling angle of $41^{\circ}43'$ of TM_0 mode is larger than those of TE modes. Experimental results of coupling angles and normalized propagation constants derived from coupling angles are shown in Table 3

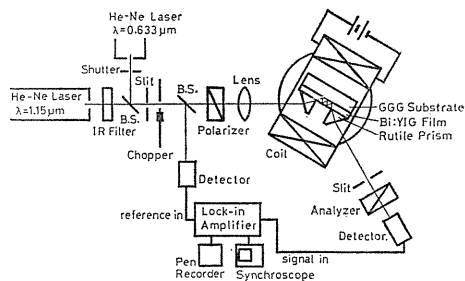


Fig. 3. Experimental set-up for the measurement of mode conversions.

As shown in Fig. 4, the mode lines were observed on the screen with IR TV camera when TE_0 mode was excited in the garnet film. The intensities of TE_1 , TE_2 and TM_0 modes are much smaller than that of TE_0 mode. The incident TE_0 mode is scattered into the higher order modes because of inhomogeneities in the film and converted to the TM_0 mode by residual magnetization of the Bi:YIG thin-film. The rutile prism is anisotropic and the optical axis is parallel to polarization direction of TE modes. Since the extraordinary refractive index for TE modes is larger

Table 3. Coupling angles and normalized propagation constants.

| Mode | Coupling angle θ (deg.) | Normalized propagation constant β/k_0 |
|---------------|-----------------------------------|--|
| TE_0 | 22.23 | 2.176 |
| TE_1 | 18.90 | 2.143 |
| TE_2 | 12.83 | 2.078 |
| TE_3 | 5.87 | 1.998 |

4. 1. Propagation Losses

By moving the output prism, the optical intensity of TE_0 mode was measured for several propagation lengths as shown in Fig. 5. The propagation loss of TE_0 mode is estimated to be 2.3 dB/mm. The output intensity of TE_0 mode seems to decrease due to the scattering into the higher order modes rather than the absorption of the Bi:YIG film. This propagation loss is also derived by the unstable coupling between the prism and the thin-film.

By fabricating Bi:YIG thin-films under the suitable sputtering conditions, the propagation loss can be reduced as small as YIG (8 dB/cm)¹⁰⁾ or less.

4. 2. Mode Conversions due to Faraday Effects

The optical effects of TE to TM mode conversion were observed as shown in Fig. 6, by applying the external magnetic field of $H_s=100$ Oe parallel to the propagation direction of the optical wave with a coil. The mode conversion efficiency of 70% has been obtained in the propagation length of 1.5 mm. The value of saturation field H_s is about 100 Oe and at the external magnetic field $H=H_s$, magnetization of the Bi:YIG film is saturated. However, the magnetic field is almost saturated at a few Oersteds.

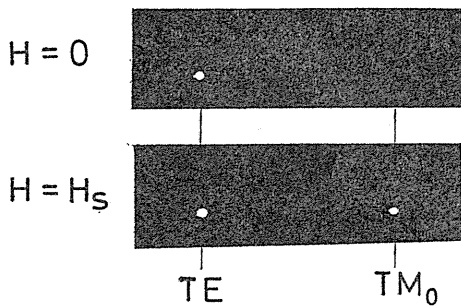


Fig. 6. TE to TM mode conversion observed with IR TV camera.

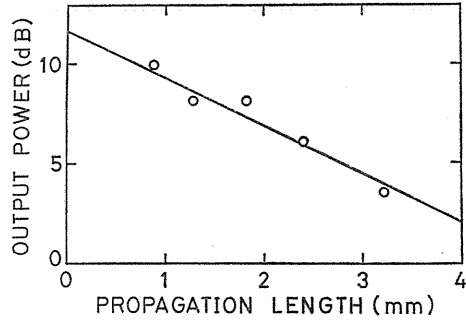


Fig. 5. Attenuation of the guided TE_0 mode.

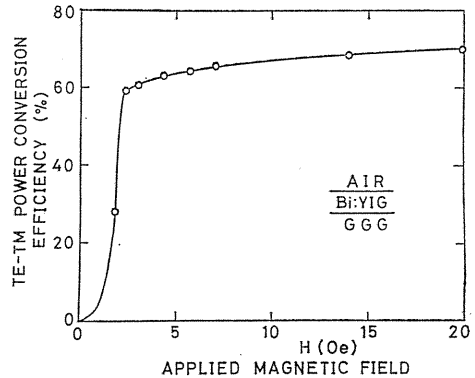


Fig. 7. Mode conversion efficiency due to the Faraday effect vs the applied magnetic field.

The magnetic field dependence of TE-TM mode conversion is shown in Fig. 7. From this result, it is found that the magnetic field required for the Faraday rotation is about only 5 Oe. Bi:YIG thin-films fabricated by RF sputtering method have magnetic anisotropy with the easy axis parallel to the film plane and their coercive force is 3 Oe. Hence, the nonreciprocal circuits for optical isolators can

be realized by very small external magnetic fields.

The TE-TM mode conversion efficiency through the Faraday effect changes sinusoidally with the propagation length as shown in Fig. 8.¹¹⁾ The maximum mode conversion efficiency, $|S|^2_{\max}$, is 75% and the minimum distance for achieving the maximum conversion, l_{\min} , is 1.65mm. The broken line was derived by substituting $|S|^2_{\max}=0.75$ and $l_{\min}=1.65$ mm into the mode conversion coefficient for the length l given by

$$|S|^2 = |S|^2_{\max} \sin^2\left(\frac{\pi}{2l_{\min}} \cdot l\right) \quad (1)$$

These results of Fig. 8 are different from the theoretical values, calculated with the assumption that Bi:YIG thin-films are isotropic.^{9,11)} If thin-film is isotropic, theoretically, specific Faraday rotation θ_F , and l_{\min} must be 3600 deg/cm and 0.22 mm, respectively, when $|S|^2_{\max}=0.75$. Therefore, it seems that Bi:YIG thin-films sputtered on GGG substrate have weak birefringences which arise from the stresses caused by the lattice misfits between the thin-films and substrates. The TE-TM mode conversion efficiency is strongly affected by the birefringence in the garnet film, so that we discuss these effects in detail in the next chapter. From Fig. 8, it is found that the TE-TM mode conversions of more than 50% can be achieved in the Bi:YIG films of thickness $W=2.13 \mu\text{m}$ without ZnO top layers that approximately satisfy the phase matching condition. Therefore, it is found that the nonreciprocal circuit can be realized with Bi:YIG thin-film of 1 mm in length without matching top layer, because the 50% mode conversion can be obtained in the short length of 1 mm.

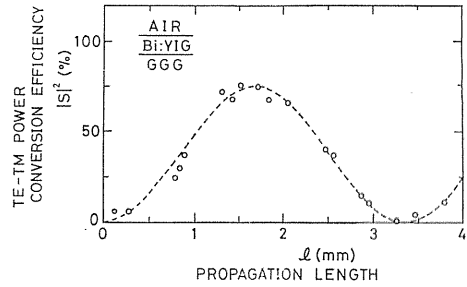


Fig. 8. Mode conversion efficiency due to the Faraday effect as a function of the propagation length.

4. 3. Mode Conversions due to Cotton-Mouton Effects

The reciprocal mode conversions due to the Cotton-Mouton effects were measured by using an electromagnet with two poles. The direction of the applied magnetic field is perpendicular to the propagation direction of the optical wave and oriented θ away from the line normal to the film plane. Figure 9 shows the reciprocal TE-TM mode conversion efficiency when $\theta=22.5^\circ$, 30° and 45° , where the magnetic field is about 150 Oe. The broken lines are estimated from Eq. (1), where $|S|^2_{\max}$ and l_{\min} are obtained for each θ , as follows.

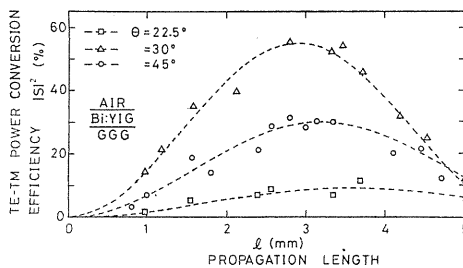


Fig. 9. Mode conversion efficiency due to the Cotton-Mouton effect as a function of the propagation length.

$$\begin{aligned} \text{for } \theta=45^\circ, & \quad |S|^2_{\text{max}}=0.30, \quad l_{\text{min}}=3.2 \text{ mm} \\ \text{for } \theta=30^\circ, & \quad |S|^2_{\text{max}}=0.55, \quad l_{\text{min}}=2.9 \text{ mm} \\ \text{for } \theta=22.5^\circ, & \quad |S|^2_{\text{max}}=0.09, \quad l_{\text{min}}=3.6 \text{ mm} \end{aligned}$$

From these results, it is found that mode conversion efficiency of 50% can be achieved for the propagation length of 2.3 mm and $\theta=30^\circ$ in the Bi:YIG thin-film of thickness $2.13 \mu\text{m}$. Hence, the reciprocal circuit of 50% conversion can be constructed with the length of 2.3 mm.

The mode conversion efficiencies due to the Cotton-Mouton effect were obtained for various intensities of the magnetic fields. Fig. 10 shows mode conversion dependence on external magnetic field for $l=2.3 \text{ mm}$ and $\theta=45^\circ$. The mode conversion efficiency becomes constant when the applied external field intensity is larger than 70 Oe. Therefore, the magnetic field required for the reciprocal circuit in the optical isolator is 70 Oe which is about ten times as large as that for the nonreciprocal circuit, because the easy magnetization axis is parallel to the film.

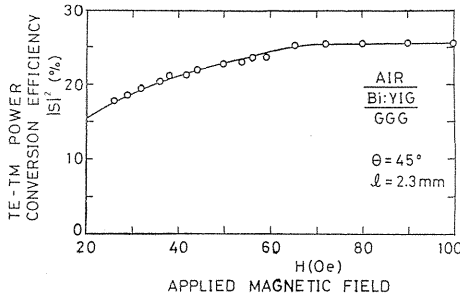


Fig. 10. Conversion dependence on external magnetic field.

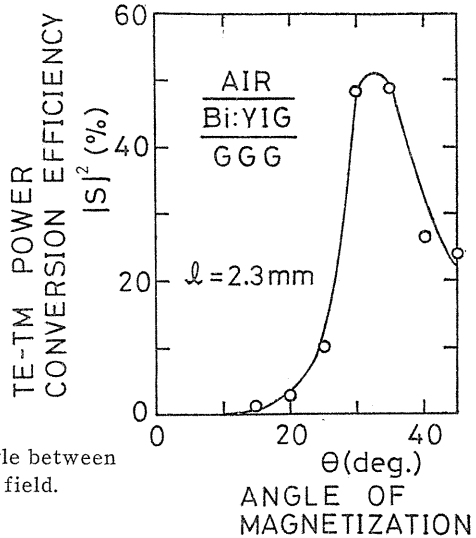


Fig. 11. Conversion dependence on angle between the normal line and magnetic field.

Fig. 11 shows the mode conversion efficiency when the direction of the applied magnetic field of 150 Oe is rotated in the plane perpendicular to the optical propagation direction.

The mode conversion efficiency is not maximum at $\theta=45^\circ$, because the magnetization of the film is not perfectly parallel to the direction of the applied magnetic field, but it tilts toward the film plane.

5. Optical Isolation in the Bi:YIG Film Waveguide

From the experimental results of non-reciprocal and reciprocal properties, the waveguide type optical isolator was constructed as shown in Figs. 12 (a) and (b), where \vec{M} is magnetization. The magnetic fields were applied with the Ba ferrite

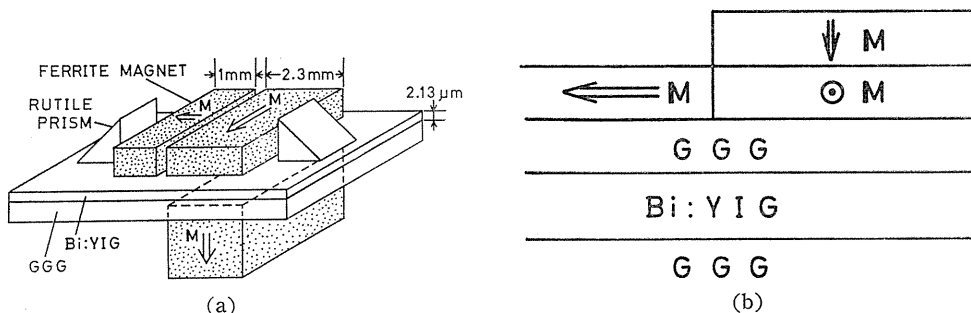


Fig. 12. Structure of the waveguide type optical isolator constructed experimentally.

magnets and the length of nonreciprocal and reciprocal parts were 1.0 and 2.3 mm, respectively. The top layer is air. The isolator operation was confirmed by reversing the direction of the magnetic fields. As mode selectors, polarizers were used at the input and output of the optical isolator. The guided mode selectors have not been sputtered on the substrates. The isolation ratio was obtained for several propagation lengths by measurement of optical output, reversing the magnetic field direction. The experimental results are shown in Fig. 13.

The maximum isolation ratio of about 7.5 dB has been accomplished in the propagation length of 4.6 mm. Compared with the optical isolator with the YIG film,⁴⁾ the film thickness and the propagation length has been reduced to 1/2.5 and 1/3, respectively, in this isolator with the Bi:YIG film. It seems that large isolation ratio can be achieved with shorter propagation length by improving birefringence character and surface roughness of garnet films, and external ferrite construction concerned with the strength and distributions of applied magnetic fields.

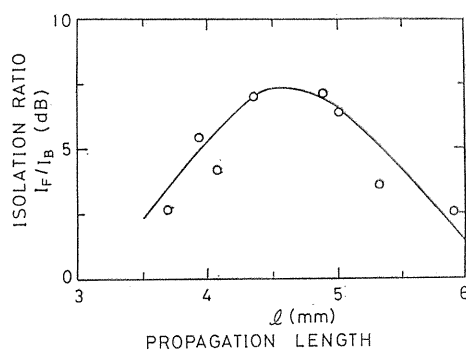


Fig. 13. Isolation ratio vs propagation length.

6. Birefringence Effects on the Mode Conversions

In order to explain the experimental results shown in Fig. 8, we discuss here the TE-TM mode conversion, assuming weak birefringences in Bi:YIG thin films, and investigate the birefringence effects on the nonreciprocal characteristics of optical isolators.¹⁶⁾

When the lattice constant of the thin film is smaller than that of the substrate, positive uniaxial anisotropy is induced in the thin film by the lattice misfit stress.^{12,17)} The specific dielectric tensor is given by

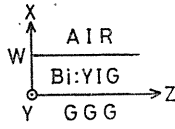
$$\tilde{\epsilon}_1 = \begin{pmatrix} \epsilon_{1x} & \epsilon_{1xy} & 0 \\ \epsilon_{1xy}^* & \epsilon_{1y} & 0 \\ 0 & 0 & \epsilon_{1z} \end{pmatrix} \quad (2)$$

$$\epsilon_{1x} = (n_1 + \Delta n_1)^2 \quad (3)$$

$$\epsilon_{1y} = \epsilon_{1z} = n_1^2 \quad (4)$$

where the z axis is the propagation direction of the optical wave and the x axis is perpendicular to the plane of the film as shown in Fig. 14. The birefringence is denoted by Δn_1 . n_1 and $n_1 + \Delta n_1$ are the refractive indices for the ordinary and extraordinary waves. The off-diagonal term ϵ_{1xy} is imaginary constant, that represents the magneto-optic effect.

Bi:YIG

$$\tilde{\epsilon}_1 = \begin{pmatrix} \epsilon_{1x} & \epsilon_{1xy} & 0 \\ \epsilon_{1xy}^* & \epsilon_{1y} & 0 \\ 0 & 0 & \epsilon_{1z} \end{pmatrix}$$


$$\epsilon_{1x} = (n_1 + \Delta n_1)^2$$

$$\epsilon_{1y} = \epsilon_{1z} = n_1^2 \quad n_1 = 2.18$$

GGG $n_2 = 1.945$

AIR $n_3 = 1.0$

Fig. 14. Birefringence effects and dielectric tensor.

The asterisk expresses complex conjugation. The refractive indices of gyrotropic thin films at wave-length of $1.15 \mu\text{m}$ are $n_1 = 2.18$ and $n_2 = 1.945$ for the Bi:YIG film and the GGG substrate. That of air top layer is $n_3 = 1.0$

Based on the unperturbed mode functions for TE and TM modes in the anisotropic films, where different diagonal terms of the dielectric tensor express birefringences and off-diagonal terms concerned with magneto-optic effects, are zero, TE-TM mode conversions can be analyzed by perturbation method, if off-diagonal terms are small perturbation parameters.

The mode conversion factor $|S|_{\text{max}}^2$ and $C = \frac{\pi}{2l_{\text{min}}}$ in eq.(1) are

$$|S|_{\text{max}}^2 = \frac{1}{1 + \left(\frac{\delta}{K}\right)^2} \quad (5)$$

and

$$C = \beta_m K \sqrt{1 + \left(\frac{\delta}{K}\right)^2} \quad (6)$$

where

$$\beta_m = \frac{K_z^{(\text{TE})} + K_z^{(\text{TM})}}{2},$$

$$\delta = \frac{K_z^{(\text{TE})} - K_z^{(\text{TM})}}{K_z^{(\text{TE})} + K_z^{(\text{TM})}}$$

$$K = \frac{|N_{12}|}{\beta_m} \quad \text{and} \quad N_{12} = \frac{1}{4} \omega \epsilon_0 \int_0^W \epsilon_{1xy}^* e_y^{(\text{TE})} e_x^{(\text{TM})} dx$$

$K_z^{(TE)}$ and $K_z^{(TM)}$, and $e_y^{(TE)}$ and $e_x^{(TM)}$ are propagation constants and fields components of the unperturbed TE and TM modes, respectively.

The birefringence factor Δn_1 changes the propagation constant $K_z^{(TM)}$. Faraday rotation θ_F is given by $\theta_F = \frac{\pi}{\lambda n} |\varepsilon_{1xy}|$. The Faraday rotation factor θ_F depends on the quantities of Bi substitution in the garnet films. $\theta_F = 280, 500, 1000, 1500$ and 2000 deg./cm correspond to $\varepsilon_{1xy} = j3.91 \times 10^{-4}, j6.98 \times 10^{-4}, j1.40 \times 10^{-3}, j2.09 \times 10^{-3}, j2.79 \times 10^{-3}$ and $j1.79 \times 10^{-3}$, respectively.

In Fig. 15, the maximum mode conversion efficiencies $|S|^2_{\max}$ are shown with regard to birefringence Δn_1 , for $k_0 W = 11.6$ ($W = 2.13 \mu\text{m}$). Mode conversions increase with θ_F . When $\Delta n_1 = 1.35 \times 10^{-3}$, $|S|^2_{\max} = 1$ and in this birefringence, the phase matching condition between TE_0 and TM_0 modes is satisfied. In Fig. 16, solid lines show the minimum distances l_{\min} where $|S|^2$ has the first maximum of $|S|^2_{\max}$ along the propagation length, and broken lines show the minimum distances l_{\min} for $|S|^2 = 0.5$. When $\Delta n_1 = 1.35 \times 10^{-3}$, l_{\min} has the maximum, while $l_{\min}^{(0.5)}$ has the minimum. l_{\min} and $l_{\min}^{(0.5)}$ decrease with θ_F .

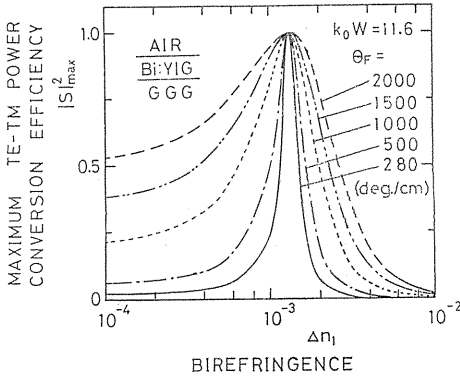


Fig. 15. Dependence of the maximum conversion efficiencies on birefringence.

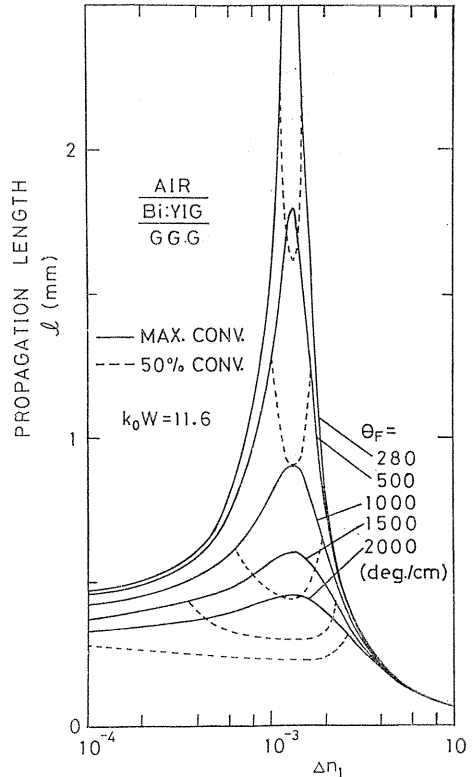


Fig. 16. The propagation length required for maximum and 50% mode conversion efficiency.

In order to estimate θ_F and Δn_1 from the experimental values of $|S|^2_{\max}$ and l_{\min} , numerical diagrams for the film thickness of $2.13 \mu\text{m}$ are shown in Fig. 17. The solid and broken lines show the conditions where $|S|^2_{\max}$ and l_{\min} are constant, respectively. The birefringence leads mode degeneracy between TE_0 and TM_0

modes in the Bi:YIG thin film when $\Delta n_1 = 1.35 \times 10^{-3}$. The minimum distance for achieving 50% mode conversion efficiency, $l_{\min}^{(0.5)}$, is minimum at phase matching point and decreases with the increase of specific Faraday rotation θ_F . The birefringence Δn_1 yields large changes of $|S|^2_{\max}$ and l_{\min} , if θ_F is small. From the experimental results of $|S|^2_{\max} = 0.75$ and $l_{\min} = 1.65$ mm for mode conversions due to Faraday effects, it can be evaluated that $\theta_F = 460$ deg./cm ($\epsilon_{1xy} = j6.0 \times 10^{-4}$) and $\Delta n_1 = 1.17 \times 10^{-3}$ for the Bi:YIG thin film sputtered on the GGG substrate.

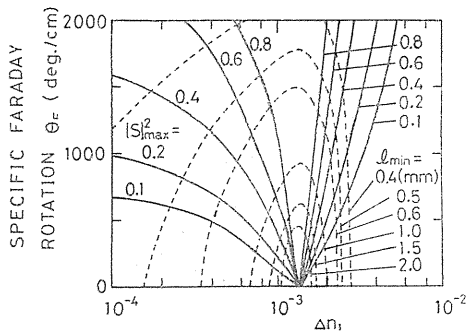


Fig. 17. Δn_1 vs θ_F for various value of $|S|^2_{\max}$ and l_{\min} .

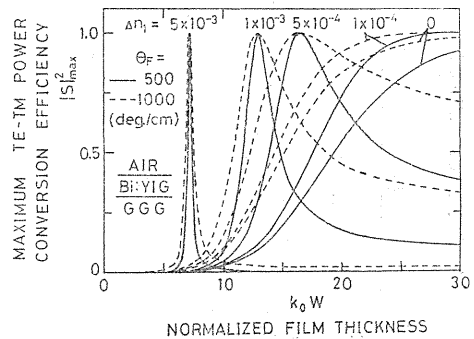


Fig. 18. The maximum mode conversion as functions of normalized film thickness.

Dependences of the maximum mode conversion efficiency $|S|^2_{\max}$ on film thickness are shown in Fig. 18, where W is the film thickness and k_0 is the free space wave number. The curves of $\Delta n_1 = 0$ correspond to the cases of isotropic films. With the increase of Δn_1 , the mode degeneracy is achieved with smaller film thickness. However, the film thickness tolerances ΔW become small in case of more than 50% mode conversion. On the other hand, ΔW becomes large as θ_F increases.

When $\Delta n_1 = 1 \times 10^{-3}$ and $\theta_F = 500$ deg./cm, $\Delta W = 0.5 \mu\text{m}$. Hence, the film thickness control can be easily accomplished in the fabrication of Bi:YIG thin films by RF sputtering method. The minimum propagation length required for $|S|^2_{\max}$ and 50% mode conversion efficiency are shown as functions of film thickness in Fig. 19. The required propagation length near mode degeneracy are constant and do not so much depend on Δn_1 , particularly, when magneto-optic effects are large, as shown in Fig. 16. Therefore, in order to reduce the propagation length of optical isolators, it is necessary to use the gyrotropic films with large magneto-optic effects. In order to fabricate optical isolators with small film thickness, it is also necessary to increase the birefringence Δn_1 .

Similarly, as for the Cotton-Mouton effect, on the assumption that, in the dielectric tensor concerned with transverse magnetic field, ϵ_{1xy} is real and other off-diagonal terms are negligible small, when $\Delta n_1 = 1.17 \times 10^{-3}$, $|S|^2_{\max}$ and l_{\min} are shown as functions of ϵ_{1xy} in Fig. 19. From the results of Fig. 20, we obtain $\epsilon_{1xy} = 1.1 \times 10^{-4}$, 3.8×10^{-4} and 2.4×10^{-4} for $\theta = 22.5$, 30 and 45°, respectively. These theoretical values are approximately equal to experimental values.

In these constructions, top layer of Bi:YIG thin film waveguides is air.

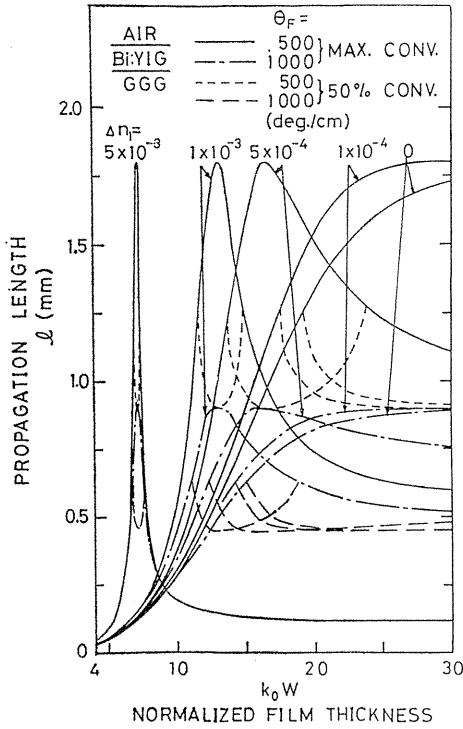


Fig. 19. Dependence of propagation length for maximum and 50% conversion efficiencies on film thickness.

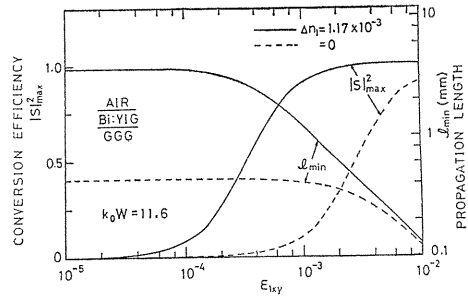


Fig. 20. The maximum lengths for Cotton-Mouton effects.

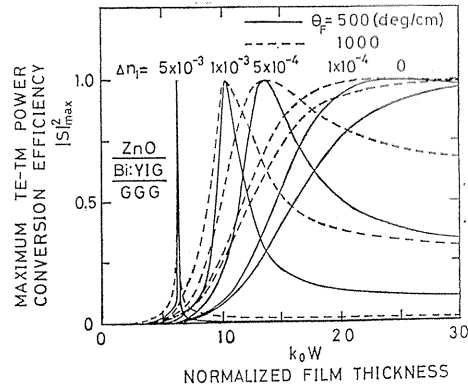


Fig. 21. The maximum mode conversions as functions of film thickness in isolators with ZnO top layer.

Finally, we consider the effects of refractive indices of top layers on mode conversions. In practice, the top layers are indispensable as buffer layers which protect guided waves from lossy effects in magnetic circuits, such as ferrites. Figs. 21 and 22 show the maximum conversion efficiencies and propagation lengths as functions of film thickness with ZnO top layer, of which refractive index $n_3=1.945$. As the refractive indices of top layers, n_3 , increase, the degenerate film thickness become small and the film thickness tolerance also becomes small, compared with the case of air top layer. The propagation length at mode degenerate film thickness, l_{min} and $l_{min}^{(0)}$, are not affected by the top layer, but dependent on θ_F of the film. The degenerate film thicknesses are evaluated for the several indices n_3 of top layer as shown in Fig. 23. From Fig. 23, it is found that the degenerate film thickness can be controlled by about $0.6 \mu\text{m}$ with the refractive index of the top layer. For example, when $\Delta n_1=1.17 \times 10^{-3}$, the complete mode conversion can be obtained with the film thickness of $2.09 \mu\text{m}$ and $n_3=1.5$ by using glass as a top layer. In these optical isolators, the propagation lengths for the nonreciprocal and reciprocal circuits reduce to 0.96 and 1.67 mm, respectively. In this case, amorphous materials can be used as top layers, so that the top layers are easily fabricated on the garnet

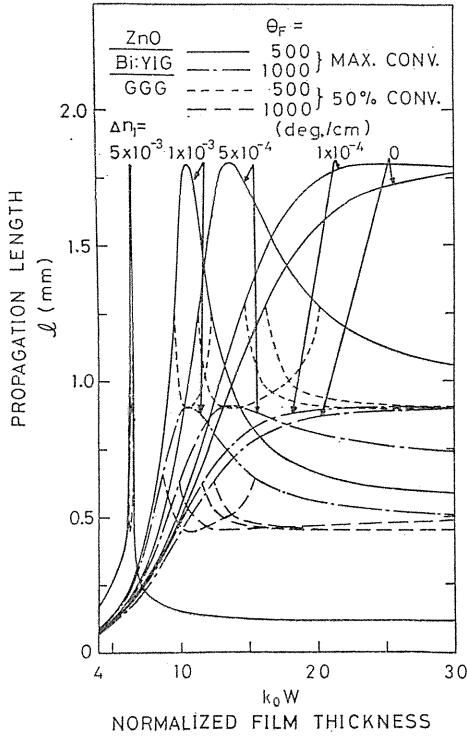


Fig. 22. Dependence of propagation length for maximum and 50% conversion efficiencies on film thickness in isolators with ZnO top layer.

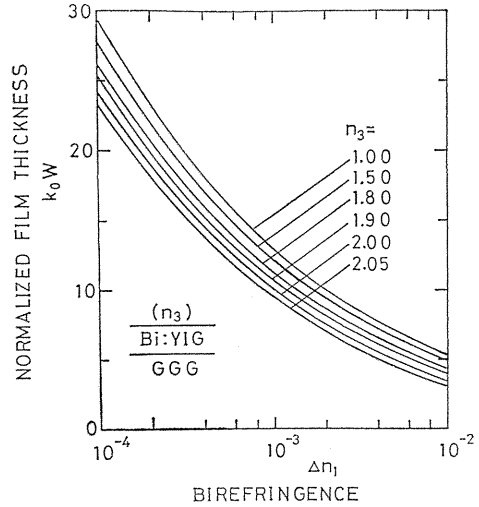


Fig. 23. The degenerate film thickness for the various n_3 .

films by RF sputtering method. Since the refractive indices of the top layers depend on the sputtering conditions, the mode degeneracy can be achieved by suitable material selection for top layers and sputtering conditions. Thin film optical isolators can be realized with small propagation length.

7. Conclusion

In order to construct waveguide type optical isolators, TE-TM mode conversions due to the Faraday and the Cotton-Mouton effects were measured in the Bi:YIG thin films sputtered on the GGG substrates. From the experimental results, it is found that there is weak birefringence of 1.17×10^{-3} in the Bi:YIG thin film, which yields useful phase matching and degenerate condition. The design data for the nonreciprocal and reciprocal circuits have been obtained at thickness of $2.13 \mu\text{m}$. The required propagation lengths and applied magnetic fields are 1 mm and 5 Oe for the nonreciprocal circuit, and 2.3 mm and 70 Oe for the reciprocal circuit. The waveguide type optical isolator consisting of the Bi:YIG thin film on the GGG substrate has been constructed with the ferrite magnets, and the isolator operation

has been confirmed. The maximum isolation ratio of 7.5 dB has been realized for the propagation length of 4.6 mm. Though this isolation ratio is not sufficient for practical use, higher isolation ratios can be achieved by controlling the strength and distributions of the magnetic fields and the propagation length under the optimum conditions concerned with top layers.

The mode degeneracy induced by the birefringence of Bi:YIG films can be applied for the fabrication of waveguide type optical isolators with high isolation ratios and low insertion losses. The degenerate film thickness can be changed by about $0.6 \mu\text{m}$ with the refractive indices of top layers. Therefore, it is necessary to select the materials which have the refractive indices suitable for top layers, considering film thickness. Moreover, it is important to fabricate the garnet films with high magneto-optic effects by modifying the substitution ratios of Bi and Al. This waveguide type optical isolator may be improved by constructing the mode selectors and the magnetizing circuits in forms of film waveguides.

Acknowledgement

The authors wish to thank Messrs. H. Ishihara and M. Yamada for many helpful discussions.

References

- 1) Agrawal, V. K., Miyazaki, Y. and Akao, Y.: "Waveguide type optical modulator using Kerr magneto-optic effects in Ni-Fe thin films: experimental study" *Jpn. J. Appl. Phys.*, **14**, (9), pp. 1313-1322 (Sept. 1975).
- 2) Tien, P. K., Martin, R. J., Wolf, R., Le Craw, R. C. and Blank, S. L.: "Switching and modulation of light in magneto-optic waveguides of garnet films" *Appl. Phys. Lett.*, **21**, (8), pp. 394-396 (Oct. 1972).
- 3) Warner, J.: "Nonreciprocal magneto-optic waveguides", *IEEE Trans. Microwave Theory & Tech.*, **MTT-23**, (1), pp. 70-78 (Jan. 1975).
- 4) Castera, J. P. and Hepner, G.: "Isolator in integrated optics using the Faraday and Cotton-Mouton effects", *IEEE Trans. Magnetics*, **MAG-13**, (5), pp. 1583-1585 (Sept. 1977).
- 5) Kitayama, K. and Kumagai, N.: "Theory and applications of coupled optical waveguides involving anisotropic or gyrotropic materials", *IEEE Trans. Microwave Theory & Tech.*, **MTT-25**, (7), pp. 567-572 (Feb. 1977).
- 6) Mitsunaga, K., Masuda, M. and Koyama, J.: "Optical waveguide isolator in Ti-diffused LiNbO_3 ", *Opt. Comm.* **27**, (3), pp. 361-364 (Dec. 1978).
- 7) Agrawal, V. K., Miyazaki, Y. and Akao, Y.: "Waveguide type optical modulator using Kerr magneto-optic effects in Ni-Fe thin films: theoretical study", *Jpn. J. Appl. Phys.*, **15**, (11), pp. 2155-2171 (Nov. 1976).
- 8) Taki, K., Miyazaki, Y. and Akao, Y.: "Optical propagation properties in gyromagnetic waveguides using Faraday effects of YIG thin films on GGG substrates", *Jpn. J. Appl. Phys.*, **19**, (5), pp. 925-938 (May 1980).
- 9) Taki, K., Miyazaki, Y. and Akao, Y.: "Optical propagation and conversion properties of hybrid modes in YIG thin-film waveguides on GGG substrates using Faraday effects with isotropic top layers", *Trans. IECE Japan*, **E 63**, (10), pp. 754-761 (Oct. 1980).

- 10) Yamada, M., Miyazaki, Y. and Akao, Y.: "Fabrication of YIG single crystal thin film by RF sputtering and fundamental properties", Paper of Technical Group, TGOQE 77-126, IECE Japan (March 1978).
- 11) Ishihara, H., Miyazaki, Y. and Akao, Y.: "Fabrication of Bi:YIG thin film waveguides by R. F. sputtering method and magneto optic conversion properties", Paper of Technical Group, TGOQE 80-76, IECE Japan (Sept. 1980).
- 12) Engen, P. G.van.: "Mode degeneracy in magnetic garnet optical waveguides with high Faraday rotation", J. Appl. Phys. 49, (9) pp. 4660-4662 (Sept. 1978).
- 13) Miyazaki, Y., Mori, M. and Akao, Y.: "Non-reciprocal and loss properties of waveguide type optical isolator using magneto optic effects in garnet crystals" Tech. Dig. 1977 Int. Conf. Integrated Optics & Optical Fiber Communication, Tokyo, p1 (A1) (1977) II-1.
- 14) Polky, J. N. and Mitchell, G. L.: "Metal-clad planar dielectric waveguide for integrated optics", J. Opt. Soc. Am. 64, (3) pp. 274-279 (March 1974).
- 15) Hepner, G., Desormiere, B. and Castera, J. P.: "Magneto optic effects in garnet thin film waveguides", Appl. Opt. 14 (7) pp. 1479-1481 (July 1975).
- 16) Yamamoto, S., Koyamada, Y. and Makimoto, T.: "Normal mode analysis of anisotropic and gyrotropic thin-film waveguides for integrated optics", J. Appl. Phys. 43 (12) pp. 5090-5097 (Dec. 1972).
- 17) Hano, M. and Kayano, H.: "Optical isolator using MBBA/YIG/GGG layered waveguide", Trans. IECE Japan, 99-C (9) pp. 215-221 (Sept. 1979).